

One-dimensional infinite chain Ag(I) complex with high quantum yield and TADF property: prepared by metal ion adjustment

Zhen-Zhou Sun, ‡^a Fu-Zhen Hu ‡^a, Cheng-Jie Gao ‡^a, Wen-Long Mou, ^a Guo Wang, ^a Ning Zhu, ^a Xun Pan, ^a Zhong-Feng Li, ^a Hong-Liang Han, ^a Hongbing Fu ^a Xiu-Lan Xin, *^b Lixiong Dai *^c Qiong-Hua Jin *^{a, d, e, f} and Qi-Ming Qiu ^g

^a Beijing Key Laboratory for Optical Materials and Photonic Devices, Department of Chemistry, Capital Normal University, Beijing 100048, China. E-mail: jinqh@cnu.edu.cn, jinqh204@163.com.

^b School of Light Industry, Beijing Technology and Business University, Beijing 100048, China.

^c Wenzhou Institute, University of Chinese Academy of Sciences, Wenzhou, 325000, China. E-mail: dailx@ucas.ac.cn.

^d State Key Laboratory of Structural Chemistry Fujian Institute of Research on the Structure of Matter, Chinese Academy of Science Fuzhou, Fujian 350002, China.

^e Key Laboratory of Advanced Energy Materials Chemistry (Ministry of Education), Nankai University, Tianjin 300071, China.

^f State Key Laboratory of Elemento-Organic Chemistry, Nankai University, Tianjin 300071, China.

^g School of Science, China University of Geosciences, Beijing 100083, China

‡These authors contributed equally to this work.

Characterization and physical measurements

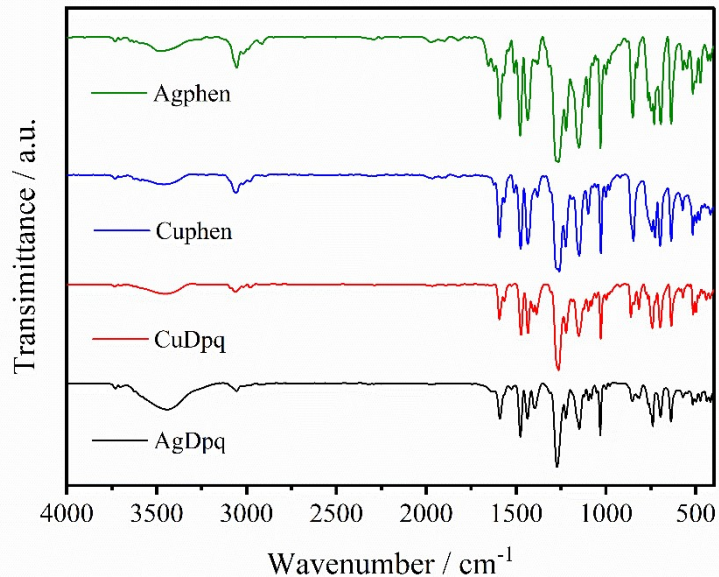


Fig. S1 The IR spectra for complexes **AgDpq**, **CuDpq**, **Agphen**, **Cuphen**.

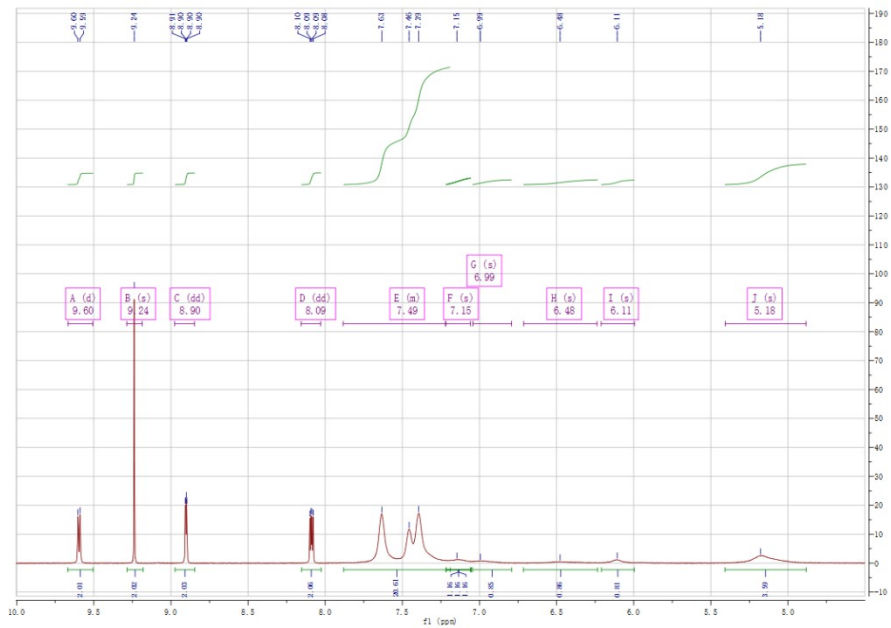


Fig. S2 ¹H NMR spectrum of **AgDpq** at room temperature.

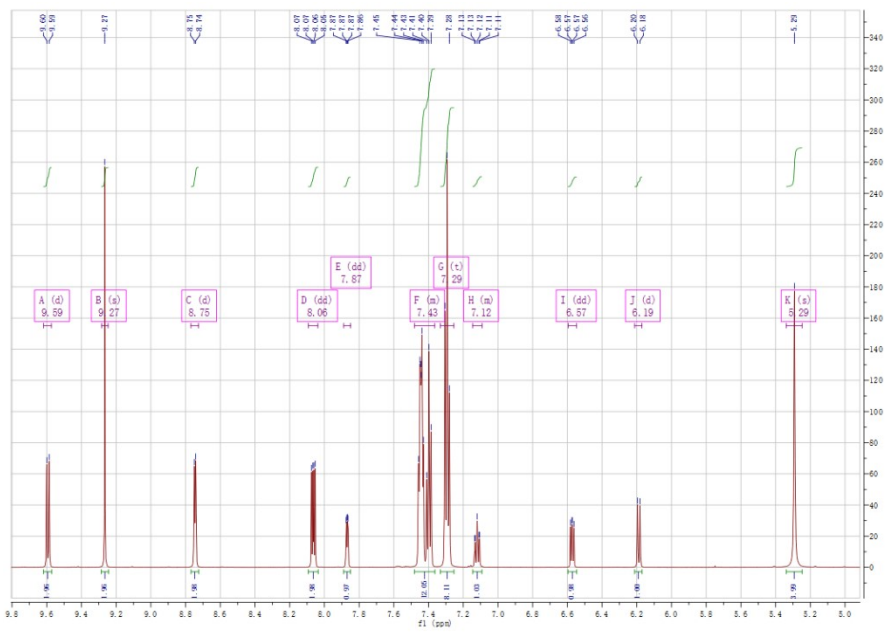


Fig. S3 ^1H NMR spectrum of **CuDpq** at room temperature.

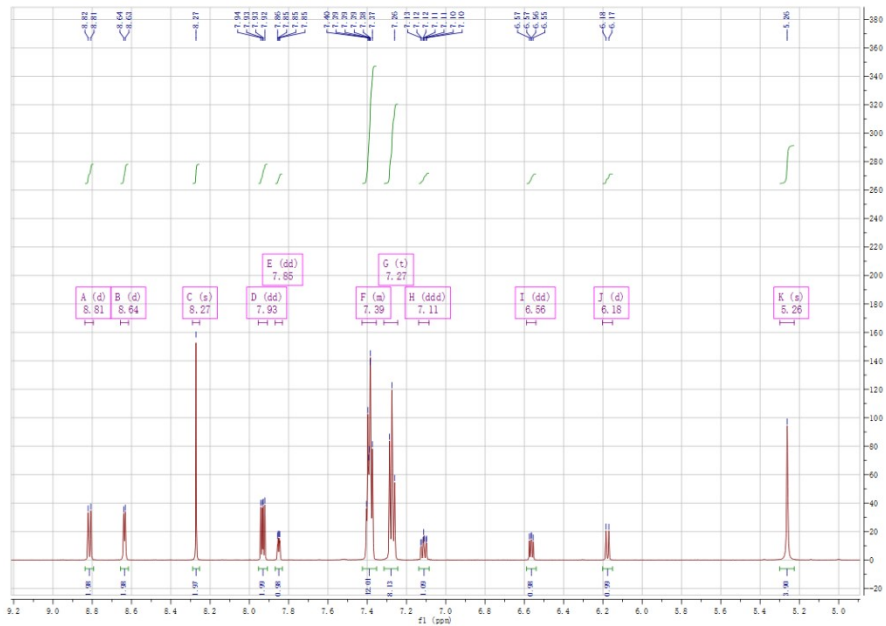


Fig. S4 ^1H NMR spectrum of **Cuphen** at room temperature.

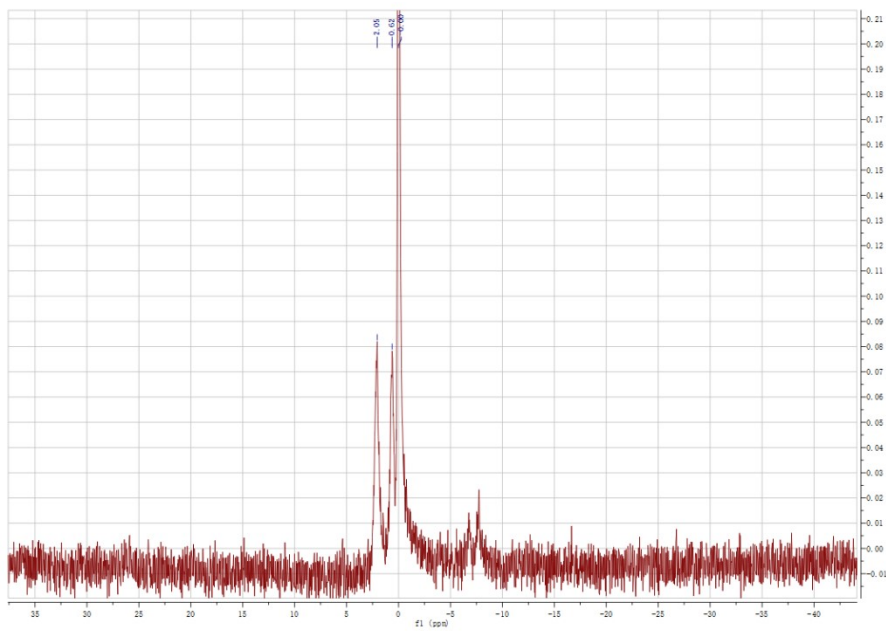


Fig. S5 ^{31}P NMR spectrum of AgDpq at room temperature.

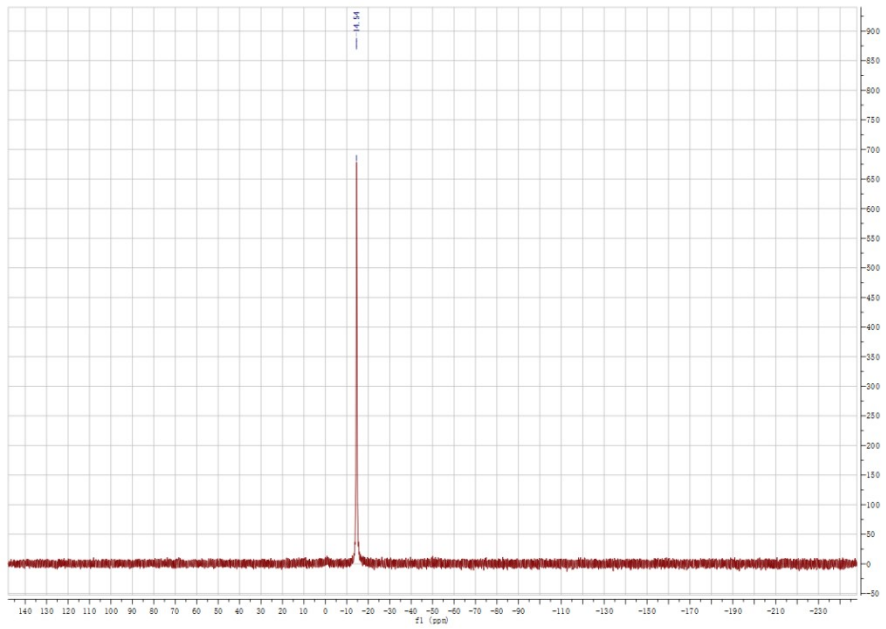


Fig. S6 ^{31}P NMR spectrum of CuDpq at room temperature.

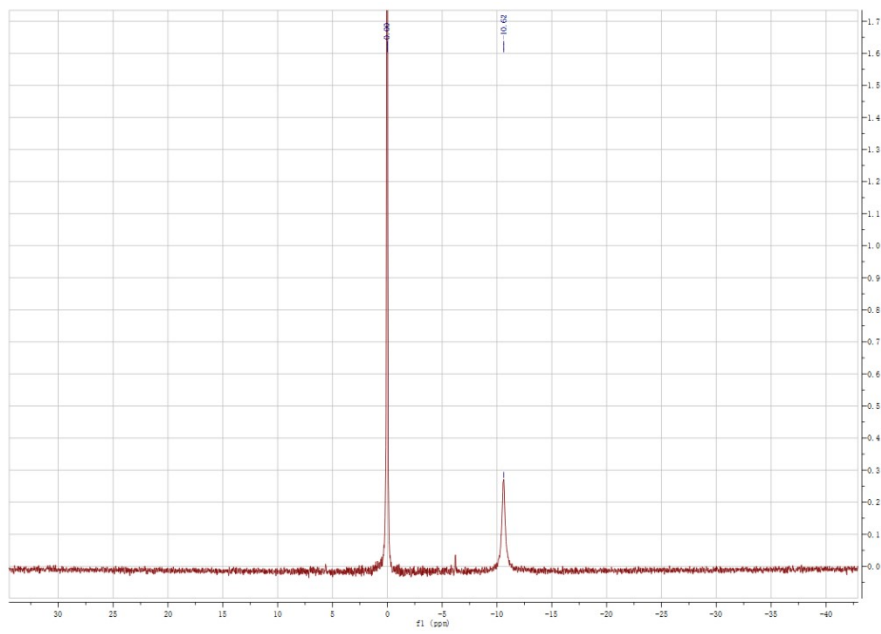


Fig. S7 ^{31}P NMR spectrum of **Cuphen** at room temperature.

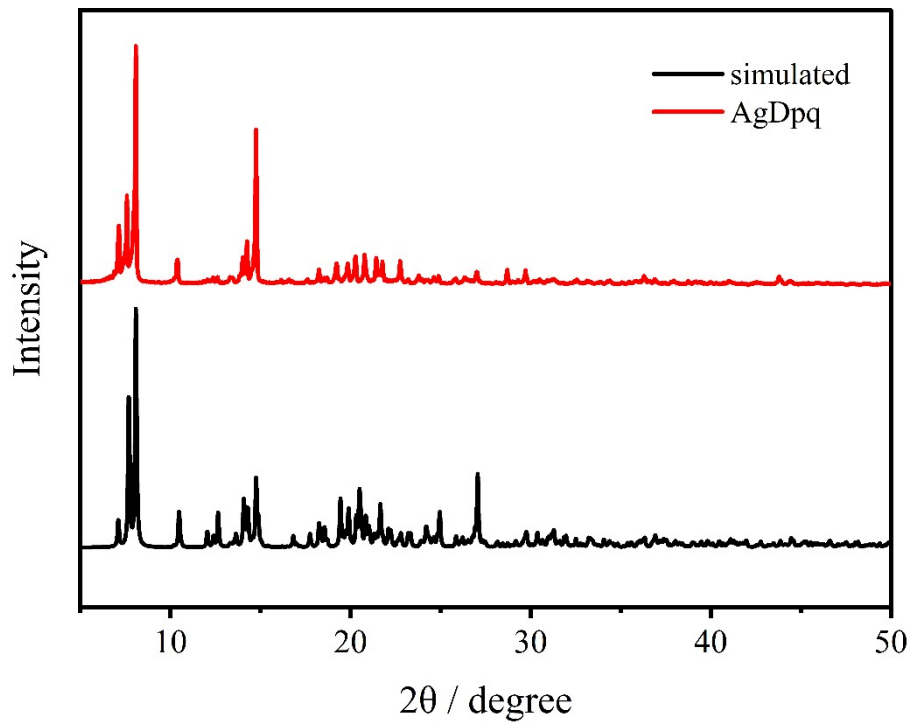


Fig. S8 The PXRD patterns for complexes **AgDpq** simulated from single crystal data (Black) and single-phase polycrystalline sample.

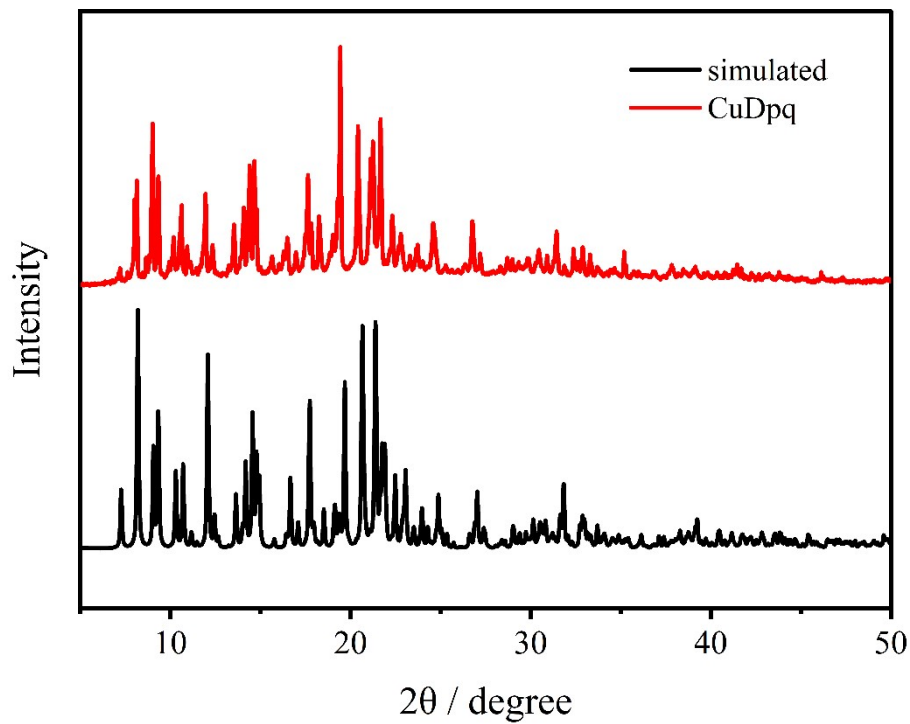


Fig. S9 The PXRD patterns for complexes **CuDpq** simulated from single crystal data (Black) and single-phase polycrystalline sample (Red).

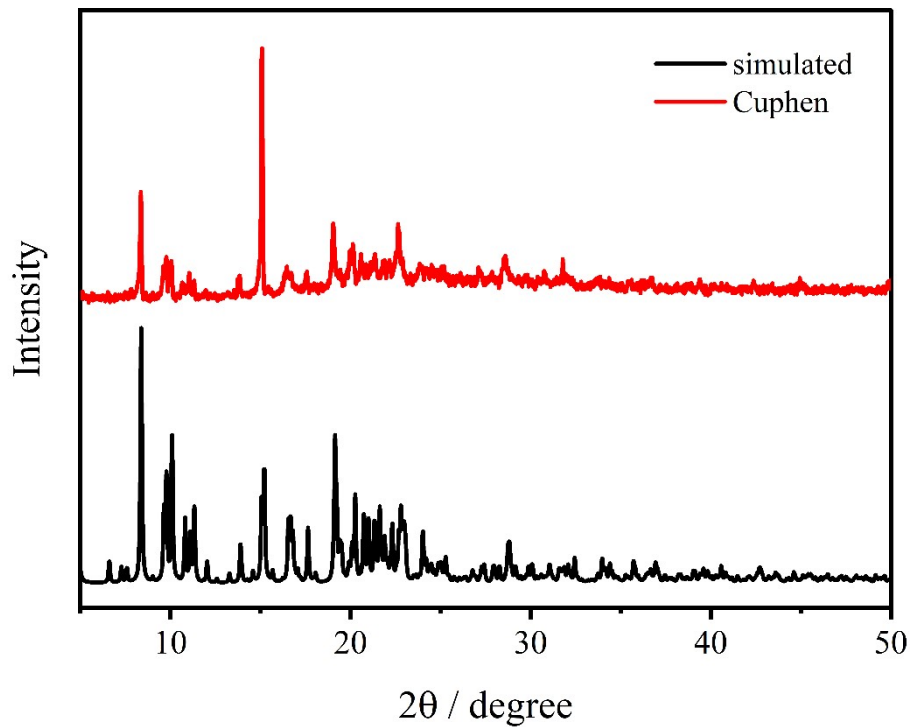


Fig. S10 The PXRD patterns for complexes **Cuphen**, simulated from single crystal data (Black) and single-phase polycrystalline sample (Red).

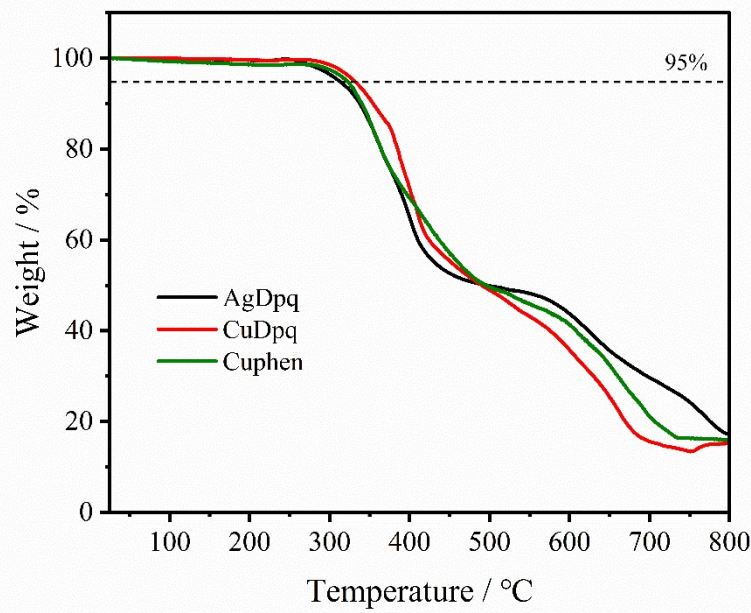


Fig. S11 Thermal stability curves for complexes **AgDpq**, **CuDpq**, **Cuphen**.

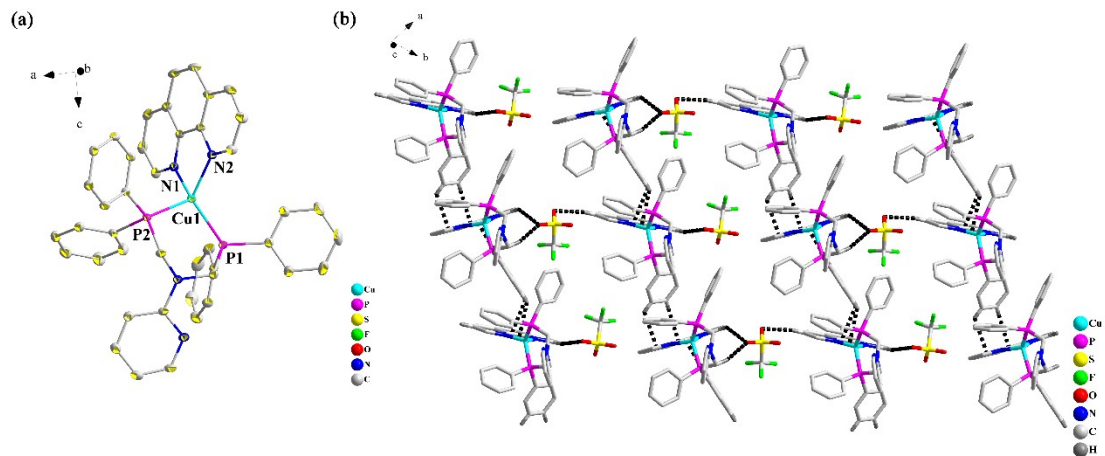


Fig. S12 (a) The structure of complex **Cuphen**. (b) The packing structure of complex **Cuphen**, including C-H \cdots π bonds (2.79, 2.79, 2.88, 2.85, and 2.91 Å), C-H \cdots O bonds (2.58, 2.43, 2.56, 2.42, 2.32, 2.35, 2.46, 2.36, 2.49, 2.37 and 2.55 Å), and Ag \cdots π (3.830, 3.791, and 3.903 Å).

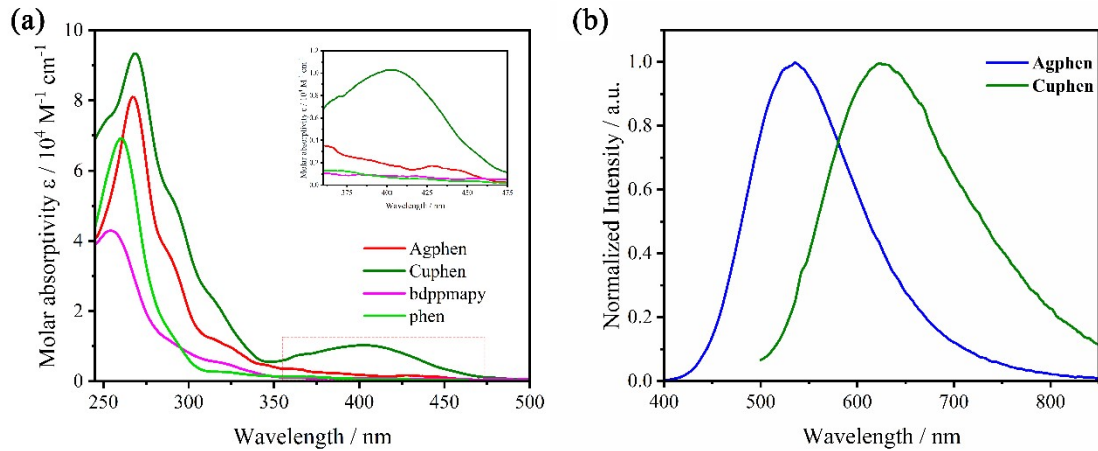


Fig. S13 (a) Absorption spectra of complexes **Agphen**, **Cuphen** and ligands. (b) Excitation spectra of **Agphen**, **Cuphen** at room temperature.

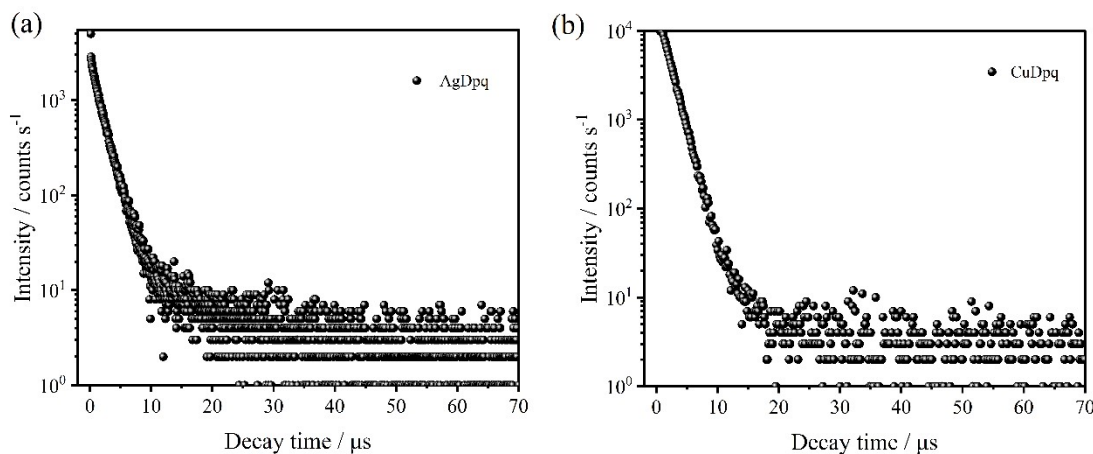


Fig. S14 (a) Emission lifetimes of **AgDpq** at room temperature. (b) Emission lifetimes of **CuDpq** at ambient temperature.

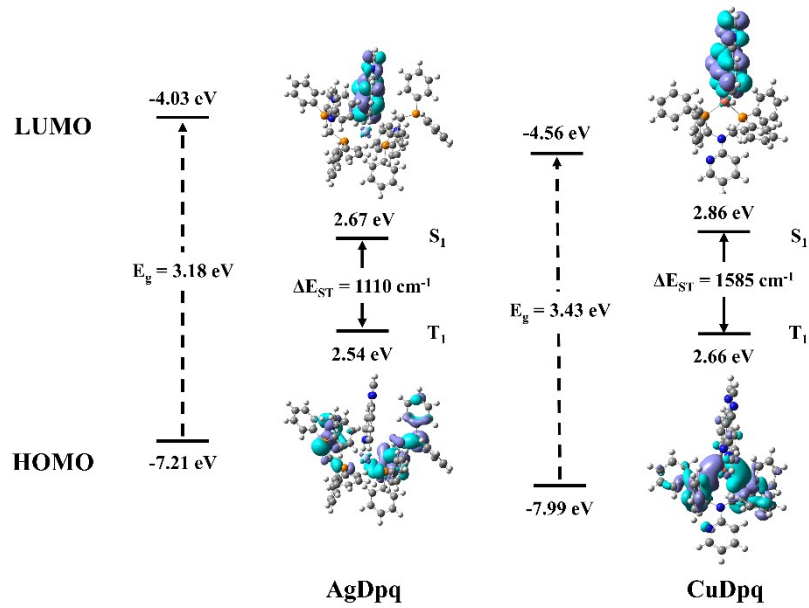


Fig. S15 HOMO and LUMO distribution and calculated frontier orbital energies, singlet (S_1), triplet (T_1) energy levels for complexes **AgDpq** and **CuDpq** based on their S_0 geometries.

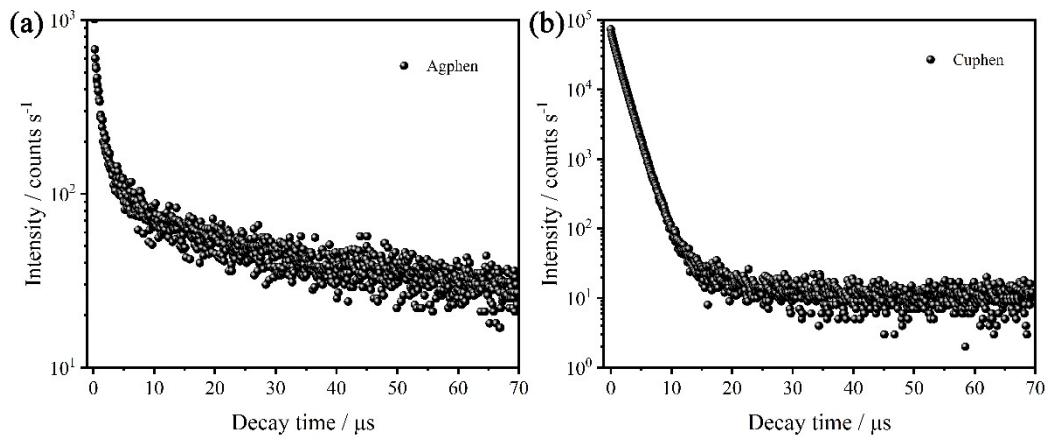


Fig. S16 (a) Emission lifetimes of **Agphen** at ambient temperature. (b) Emission lifetimes of **Cuphen** at ambient temperature.

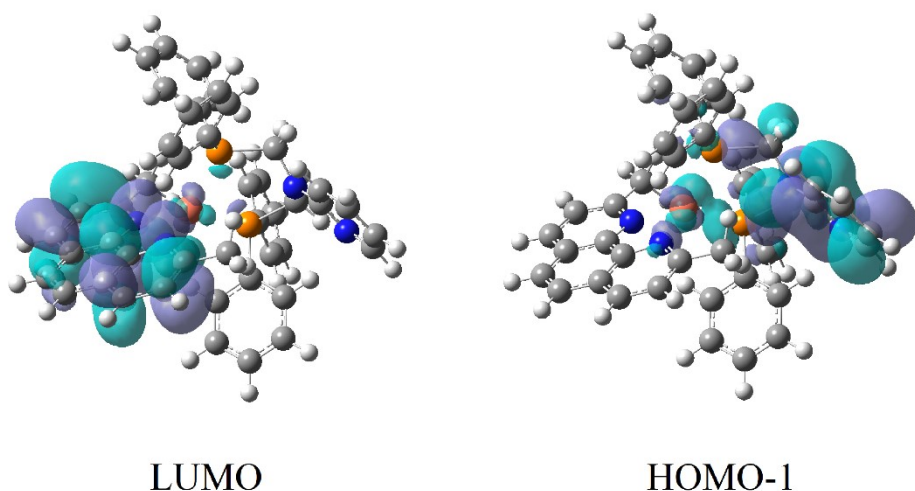


Fig. S17 Frontier MOs for singlet (S_0) states of the fully optimized **Cuphen** cation.

3. Crystallographic data

Table S1 The selected bond distances and angles for complexes.

AgDpq			
Ag(1)-P(1)	2.4444(12)	P(1)-Ag(1)-P(2)	114.89(4)
Ag(1)-P(2)	2.4609(13)	N(2)-Ag(1)-P(1)	126.90(12)
Ag(1)-N(2)	2.349(4)	N(2)-Ag(1)-P(2)	107.10(11)
Ag(1)-N(1)	2.388(4)	N(2)-Ag(1)-N(1)	70.58(14)
		N(1)-Ag(1)-P(1)	108.39(10)
		N(1)-Ag(1)-P(2)	123.04(11)

CuDpq			
Cu(1)-P(1)	2.2223(4)	P(1)-Cu(1)-P(2)	102.573(17)
Cu(1)-P(2)	2.2413(5)	N(2)-Cu(1)-P(2)	116.86(4)
Cu(1)-N(1)	2.0364(13)	N(2)-Cu(1)-P(1)	123.36(4)
Cu(1)-N(2)	2.0768(14)	N(1)-Cu(1)-P(2)	108.50(4)
		N(1)-Cu(1)-P(1)	124.18(4)
		N(1)-Cu(1)-N(2)	80.82(5)

Cuphen			
Cu(1)-P(2)	2.2442(5)	P(1)-Cu(1)-P(2)	102.458(17)
Cu(1)-P(1)	2.2223(5)	N(1)-Cu(1)-P(2)	107.94(4)
Cu(1)-N(1)	2.1077(14)	N(1)-Cu(1)-P(1)	128.69(4)
Cu(1)-N(2)	2.0274(14)	N(2)-Cu(1)-P(2)	115.59(4)
Cu(2)-P(3)	2.2537(5)	N(2)-Cu(1)-P(1)	120.68(4)
Cu(2)-P(4)	2.2442(4)	N(2)-Cu(1)-N(1)	81.18(6)
Cu(2)-N(6)	2.1026(14)	P(4)-Cu(2)-P(3)	97.388(16)
Cu(2)-N(5)	2.0522(14)	N(6)-Cu(2)-P(3)	123.09(4)
		N(6)-Cu(2)-P(4)	119.46(4)
		N(5)-Cu(2)-P(3)	110.01(4)
		N(5)-Cu(2)-P(4)	128.38(4)
		N(5)-Cu(2)-N(6)	80.76(5)

Table S2 Weak interactions for complexes.

	C-H→Cg(i)/(A)	Cg	Symmetry code	H···Cg(A) / Å
AgDpq	C26-H26→Cg(9)	C34-C35-C36-C37-C38-C39	x, y, z	2.87
	C29-H29→Cg(7)	C21-C22-C23-C24-C25-C26	1-x, 1-y, 1-z	2.67
	C33-H33A→Cg(3)	N2-C6-C7-C8-C9-C10	x, 3/2-y, 1/2+z	2.79
	C33-H33B→Cg(1)	Ag1-N1-C5-C6-N2	x, 3/2-y, 1/2+z	2.63
	C23-H23-N3	/	1-x, 1-y, 1-z	2.55
	C45-H45-O2	/	/	2.40
CuDpq	C14-H14→Cg(11)	C40-C41-C42-C43-C44-C45	1-x, -1/2+y, 1/2-z	2.97
	C17-H17→Cg(8)	C21-C22-C23-C24-C25-C26	x, 1+y, z	2.95
	C38-H38→Cg(3)	N1-C1-C2-C3-C4-C5	x, 1+y, z	2.92
	C1-H1···O1	/	-1-x, 1-y, 1-z	2.37
	C9-H9···F2	/	1-x, -1/2-y, 1/2-z	2.44
	C19-H19···O1	/	-1+x, y, z	2.52
	C33-H33A···O1	/	-1-x, 1-y, 1-z	2.56
Cuphen	C42-H42···O3	/	1-x, 1/2+y, 1/2-z	2.49
	C20-H20→Cg1	Cu1-N1-C6-C5-N2	x, y, z	2.89
	C22-H22→Cg19	C48-C49-C50-C51-C55-C56	-x, 1-y, 1-z	2.73
	C23-H23→Cg14	C7-C8-C9-C10-C12-C11	-x, 1-y, 1-z	2.70
	C71-H71→Cg3	N1-C6-C7-C8-C9-C10	1-x, -y, 1-z	2.90
	C72-H72→Cg6	C4-C5-C6-C7-C11-C12	1-x, -y, 1-z	2.64
	C1-H1···O3	/	/	2.55
	C18-H18A···O3	/	/	2.48
	C46-H46···O2	/	1-x, 1-y, 1-z	2.48
	C54-H54···O6	/	-1+x, y, z	2.40

Table S3 Compositions of HOMO and LUMO in the S₁ state of complexes **AgDpq** and **CuDpq** in the optimized S₀ structure.

	Orbital	Energy / eV	Contributions / %		
			Ag/Cu	N	P
AgDpq	LUMO+1	-4.44	1.72	94.13	4.15
	HOMO-1	-7.29	1.58	0.62	97.80
CuDpq	LUMO	-5.02	2.26	94.71	3.03
	HOMO-1	-8.23	38.77	4.83	56.40

Table S4 Energy, oscillator strength and major contribution of the calculated transitions for complexes **AgDpq**, **CuDpq** and **Cuphen**.

Excited state	Energy	Oscillator strength	Major contribution %		
			HOMO	-> LUMO	3.84
AgDpq absorption	2.6731 eV 463.83 nm	0.0085 HOMO	HOMO	-> LUMO+1	93.33
AgDpq absorption	4.8833 eV 253.89 nm	0.1590	HOMO-29 -> LUMO	11.55	
			HOMO-28 -> LUMO	17.48	
			HOMO-27 -> LUMO+1	11.58	
			HOMO-26 -> LUMO	8.64	
			HOMO-26 -> LUMO+1	3.09	
			HOMO-21 -> LUMO+2	4.91	
			HOMO-20 -> LUMO+2	6.75	
			HOMO-3 -> LUMO+5	4.70	
			HOMO-3 -> LUMO+6	2.27	
AgDpq emission	2.4002 eV 516.56 nm	0.0036 LUMO+1	LUMO+1	-> HOMO-2	3.92
CuDpq absorption	2.8562 eV 434.08 nm	0.0764 HOMO-1	HOMO-1	-> LUMO	92.42
CuDpq absorption	4.9138 eV 252.32 nm	0.5005 HOMO-18 -> LUMO+2	HOMO-18 -> LUMO+2	12.99	
			HOMO-17 -> LUMO+2	9.64	
			HOMO-16 -> LUMO+2	4.00	

			HOMO-15 -> LUMO+2	26.11
			HOMO-14 -> LUMO	14.41
			HOMO-14 -> LUMO+2	3.61
			HOMO-1 -> LUMO+5	3.14
			HOMO-1 -> LUMO+11	2.90
CuDpq	2.6263 eV	0.0974	LUMO -> HOMO-1	97.81
emission	472.08 nm			
Cuphen	4.6879 eV	0.1386	HOMO-15 → LUMO	(21.55)
absorption	264.48 nm		HOMO-15 → LUMO+1	(2.80)
			HOMO-12 → LUMO+1	(4.50)
			HOMO-5 → LUMO+1	(4.15)
			HOMO-4 → LUMO+1	(6.30)
			HOMO-3 → LUMO+2	(10.06)
			HOMO-2 → LUMO+5	(20.45)
			HOMO → LUMO+11	(10.66)
Cuphen	2.5319 eV	0.0198	HOMO-3 → LUMO	(8.03)
emission	489.69 nm		HOMO-2 → LUMO	(28.55)
			HOMO-1 → LUMO	(59.20)